Inorg. Chem. **2008**, *47*, 5727−5735

Self-Assembly of a Cyclic Metalladecapyridine from the Reaction of 2,6-Bis(bis(2-pyridyl)methoxymethane)pyridine with Silver(I)

Jie-Sheng Huang,* Jin Xie, Steven C. F. Kui, Guo-Su Fang, Nianyong Zhu, and Chi-Ming Che*

Department of Chemistry and Open Laboratory of Chemical Biology of the Institute of Molecular Technology for Drug Discovery and Synthesis, The University of Hong Kong, Pokfulam Road, Hong Kong, China

Received January 2, 2008

Reaction of $Ag(p\text{-}MeC_6H_4SO_3)$ with 2,6-bis(bis(2-pyridyl)methoxymethane)pyridine (PY5) in CH_2Cl_2 gave $[Ag^I_2(PY5)_2](p\text{-}MeC_6H_4SO_3)_2$ (**1**). Treatment of 2,6-bis(bis(2-pyridyl)hydroxymethane)pyridine (PY5-OH) with $AgNO_3$ in MeOH gave $[Ag^I_2(PY5\text{-}OH)_2](NO_3)_2$ (**2**); in the presence of PPh_3, this reaction afforded $[Ag^I(PY5\text{-}OH)(PPh_3)]NO_3$ (**3**). The structures of **1**−**3** have been determined by X-ray crystal analysis, revealing four-coordinate Ag^I ions in these complexes. Both **1** and **2** feature a quadruply branched 28-membered $C_{16}N_{10}M_2$ metallamacrocycle fused to 10 pyridyl groups. On the basis of ^1H NMR measurements, the dinuclear **1** and **2** dissociate into a mononuclear complex upon dissolving in MeCN but in MeOH an equilibrium between the mono- and dinuclear species can be detected.

Introduction

Molecules that contain multiple pyridyl groups are widely used in the design and self-assembly of metal−organic architectures.[1] In 1997, Stack,[2] Feringa,[3] and co-workers independently reported a polypyridyl ligand, 2,6-bis(bis(2-pyridyl)methoxymethane)pyridine (PY5), which has five pyridyl subunits arranged like a crab (Chart 1). This PY5 "crab" has been demonstrated, as in the elegant works by Stack and co-workers,[2,4] to be a unique mononucleating chelator for a series of first-row transition-metal ions, from $Mn^{II,III}$, $Fe^{II,III}$, Co^{II}, Ni^{II}, Cu^{II}, to Zn^{II}, resulting in the formation of mononuclear six-coordinate metal complexes **I** (Chart 1) that exclusively contain PY5 in a pentadentate coordination mode, except for $[Cu^{II}(PY5)Cl]Cl$[4b] (**II**, Chart 1), adopting a tetradentate coordination mode of PY5. In our efforts to develop the synthetic chemistry of PY5 complexes of ruthenium, which involved the use of $Ag(p\text{-}MeC_6H_4SO_3)$, we found that PY5 and its congener PY5-OH[2,3] (2,6-bis(bis(2-pyridyl)hydroxymethane)pyridine, Chart 1)[5] readily reacted with Ag^I to afford two new types of metal PY5 or PY5-OH complexes **III** and **IV** (Chart 1) that contain PY5 or PY5-OH ligands in a tridentate and bridging tetradentate coordination mode, respectively. A tridentate coordination mode of a closely related ligand 2,6-bis(1,1-bis(2-pyridyl)-ethyl)pyridine (PY5-Me, Chart 1) was previously proposed by Canty and co-workers for the Pd^{II} complex $[Pd^{II}(PY5\text{-}Me)(OAc)](OAc)\cdot 3H_2O$,[6] the structure of which has not been determined by X-ray crystal analysis. No other examples of metal PY5-Me complexes have been reported.

* To whom correspondence should be addressed. E-mail: jshuang@hkucc.hku.hk (J.S.H.), cmche@hku.hk (C.M.C.).

(1) For reviews, see: (a) Lawrence, D. S.; Jiang, T.; Levett, M. *Chem. Rev.* **1995**, *95*, 2229–2260. (b) Linton, B.; Hamilton, A. D. *Chem. Rev.* **1997**, *97*, 1669–1680. (c) Blake, A. J.; Champness, N. R.; Hubberstey, P.; Li, W.-S.; Withersby, M. A.; Schröder, M. *Coord. Chem. Rev.* **1999**, *183*, 117–138. (d) Leininger, S.; Olenyuk, B.; Stang, P. J. *Chem. Rev.* **2000**, *100*, 853–907. (e) Swiegers, G. F.; Malefetse, T. J. *Chem. Rev.* **2000**, *100*, 3483–3537. (f) Ward, M. D.; McCleverty, J. A.; Jeffery, J. C. *Coord. Chem. Rev.* **2001**, *222*, 251–272. (g) Greig, L. M.; Philp, D. *Chem. Soc. Rev.* **2001**, *30*, 287–302. (h) Mamula, O.; von Zelewsky, A. *Coord. Chem. Rev.* **2003**, *242*, 87–95. (i) Piguet, C.; Borkovec, M.; Hamacek, J.; Zeckert, K. *Coord. Chem. Rev.* **2005**, *249*, 705–726. (j) Thanasekaran, P.; Liao, R.-T.; Liu, Y.-H.; Rajendran, T.; Rajagopal, S.; Lu, K.-L. *Coord. Chem. Rev.* **2005**, *249*, 1085–1110. (k) Vriezema, D. M.; Aragonès, M. C.; Elemans, J. A. A. W.; Cornelissen, J. J. L. M.; Rowan, A. E.; Nolte, R. J. M. *Chem. Rev.* **2005**, *105*, 1445–1489.

(2) Jonas, R. T.; Stack, T. D. P. *J. Am. Chem. Soc.* **1997**, *119*, 8566–8567.

(3) de Vries, M. E.; La Crois, R. M.; Roelfes, G.; Kooijman, H.; Spek, A. L.; Hage, R.; Feringa, B. L. *Chem. Commun.* **1997**, 1549–1550.

(4) (a) Goldsmith, C. R.; Jonas, R. T.; Stack, T. D. P. *J. Am. Chem. Soc.* **2002**, *124*, 83–96. (b) Gebbink, R. J. M. K.; Jonas, R. T.; Goldsmith, C. R.; Stack, T. D. P. *Inorg. Chem.* **2002**, *41*, 4633–4641. (c) Goldsmith, C. R.; Jonas, R. T.; Cole, A. P.; Stack, T. D. P. *Inorg. Chem.* **2002**, *41*, 4642–4652. (d) Goldsmith, C. R.; Cole, A. P.; Stack, T. D. P. *J. Am. Chem. Soc.* **2005**, *127*, 9904–9912. (e) Goldsmith, C. R.; Stack, T. D. P. *Inorg. Chem.* **2006**, *45*, 6048–6055.

(5) Only one metal PY5-OH complex, $[Fe^{II}(PY5\text{-}OH)Cl](CF_3SO_3)$, has previously been structurally characterized, which adopts the type-**I** structure in Chart 1. See : Wong, E. L.-M.; Fang, G.-S.; Che, C.-M.; Zhu, N. *Chem. Commun.* **2005**, 4578–4580.

(6) Canty, A. J.; Minchin, N. J.; Skelton, B. W.; White, A. H. *J. Chem. Soc., Dalton Trans.* **1986**, 2205–2210.

10.1021/ic8000043 CCC: $40.75
Published on Web 06/13/2008

Chart 1

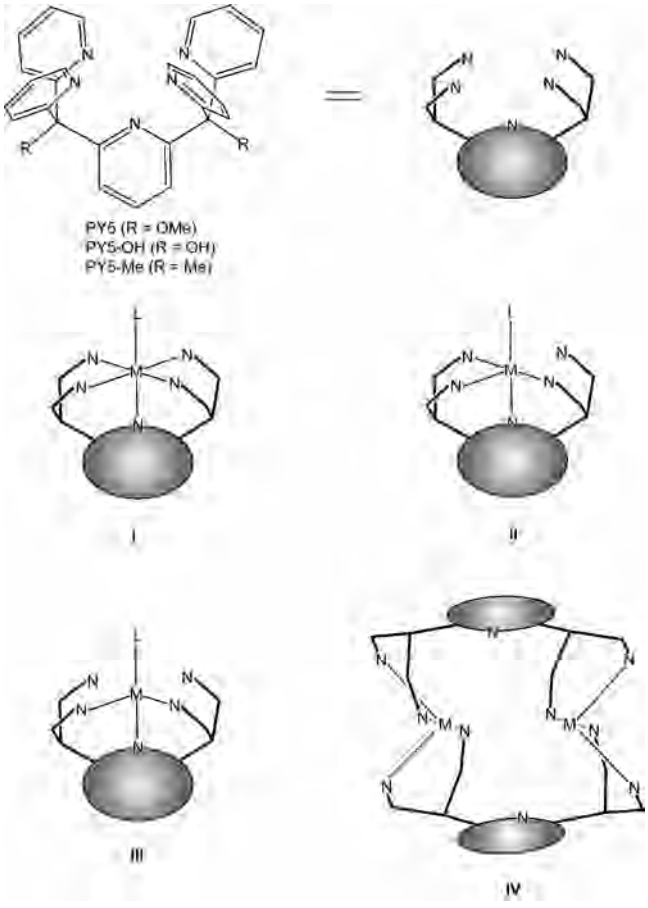

Herein are described the isolation, X-ray crystal structure, and solution behavior of the new types of metal complexes containing PY5 or PY5-OH ligand (**III** and **IV**). Whereas the formation of mononuclear species **III** at the expense of uncoordination of two 2-pyridyl groups further highlights the mononucleating property of PY5 or PY5-OH, the isolation of **IV** is the first example where a member of the family of the PY5 crab and its congeners[7] chelates more than one metal ion and functions as a binucleating chelator, leading to the isolation of a unique cyclic metalladecapyridine.

Results and Discussion

Synthesis. Treatment of a solution of PY5 in MeOH with a solution of $Ag(p\text{-}MeC_6H_4SO_3)$ (1 equiv) in CH_2Cl_2 for 30 min followed by recrystallization of the crude product from CH_2Cl_2/MeOH/Et_2O afforded $[Ag^I_2(PY5)_2](p\text{-}MeC_6H_4SO_3)_2$ (**1**) in 90% yield. The reaction of PY5-OH and $AgNO_3$ (1 equiv) in MeOH, with subsequent recrystallization from MeOH/Et_2O, gave $[Ag^I_2(PY5\text{-}OH)_2](NO_3)_2$ (**2**) (yield: 90%). In the presence of PPh_3 (1 equiv), PY5-OH reacted with $AgNO_3$ (1 equiv) in MeOH to afford $[Ag^I(PY5\text{-}OH)(PPh_3)]NO_3$ (**3**) in 88% yield. The synthetic routes to **1**−**3** are depicted in Scheme 1.

(7) Besides PY5-OH and PY5-Me, another PY5 congener, 2,6-bis(bis(2-pyridyl)methyl)pyridine (PY5-H), was reported recently but has not been employed in metal complex formation. See: Dyker, G.; Muth, O. *Eur. J. Org. Chem.* **2004**, 4319–4322.

Scheme 1

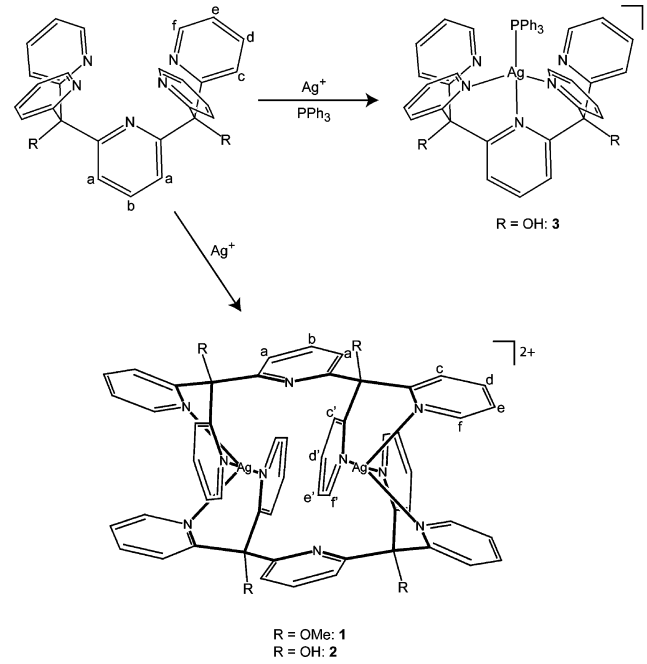

1−**3** are air-stable white solids, which are soluble in MeCN. **1** and **3** are soluble in MeOH as well, but a markedly lower solubility of **2** in MeOH was observed.

Given the well-documented six-coordinate structure **I** usually adopted by metal PY5 or PY5-OH complexes and the previous reports of a number of six-coordinate Ag^I complexes in the literature,[8] the formation of **1**−**3** that adopt the four-coordinate structures **III** and **IV** is somewhat interesting. In literature, the generation of mononuclear four-coordinate metal complexes from a multidentate ligand that usually affords mononuclear six-coordinate metal complexes is not unprecedented. For example, Schröder and co-workers reported that 1,4,10,13-tetrathia-7,16-diazacyclo-octadecane ([18]aneN_2S_4) generally forms six-coordinate complexes $[M([18]aneN_2S_4)]^{n+}$ with Ni^{II}, Cu^{II}, Fe^{II}, Hg^{II}, Co^{III}, or Rh^{III} but forms an essentially four-coordinate complex $[Pd([18]aneN_2S_4)]^{2+}$ with Pd^{II}.[9a,b] A different behavior of [18]aneN_2S_4, compared with PY5 or PY5-OH, lies in the formation of $[Ag^I([18]aneN_2S_4)]^+$ that still adopts a six-coordinate structure.[9c]

X-ray Crystal Structures. We obtained diffraction-quality crystals of **1**·2MeOH, **2**, and **3**·3.5H_2O by slow diffusion of Et_2O into their MeOH solutions. A diffraction-quality

(8) For examples, see: (a) Clarkson, J.; Yagbasan, R.; Blower, P. J.; Rawle, S. C.; Cooper, S. R. *J. Chem. Soc., Chem. Commun.* **1987**, 950–951. (b) Blower, P. J.; Clarkson, J. A.; Rawle, S. C.; Hartman, J. R.; Wolf, R. E., Jr.; Yagbasan, R.; Bott, S. G.; Cooper, S. R. *Inorg. Chem.* **1989**, *28*, 4040–4046. (c) de Groot, B.; Jenkins, H. A.; Loeb, S. J. *Inorg. Chem.* **1992**, *31*, 203–208. (d) Blake, A. J.; Gould, R. O.; Parsons, S.; Radek, C.; Schröder, M. *Angew. Chem., Int. Ed. Engl.* **1995**, *34*, 2374–2376. (e) Hirsch, K. A.; Wilson, S. R.; Moore, J. S. *Inorg. Chem.* **1997**, *36*, 2960–2968. (f) Blake, A. J.; Gould, R. O.; Li, W.-S.; Lippolis, V.; Parsons, S.; Radek, C.; Schröder, M. *Inorg. Chem.* **1998**, *37*, 5070–5077. (g) Côté, A. P.; Shimizu, G. K. H. *Inorg. Chem.* **2004**, *43*, 6663–6673.

(9) (a) Reid, G.; Blake, A. J.; Hyde, T. I.; Schröder, M. *J. Chem. Soc., Chem. Commun.* **1988**, 1397–1399. (b) Reid, G.; Schröder, M. *Chem. Soc. Rev.* **1990**, *19*, 239–269. (c) Blake, A. J.; Reid, G.; Schröder, M. *J. Chem. Soc., Dalton Trans.* **1991**, 615–620.

Table 1. Crystallographic Data of **1**·2MeOH, **1**·2H_2O, **2**, and **3**·3.5H_2O

	1·2MeOH	**1**·2H_2O	**2**	**3**·3.5H_2O
formula	$C_{72}H_{64}Ag_2N_{10}O_{10}S_2$·2MeOH	$C_{72}H_{64}Ag_2N_{10}O_{10}S_2$·2$H_2O$	$C_{54}H_{42}Ag_2N_{12}O_{10}$	$C_{45}H_{36}AgN_6O_5P$·3.5H_2O
cryst syst	triclinic	triclinic	triclinic	triclinic
fw	1573.28	1545.22	1234.74	942.69
space group	$P\bar{1}$	$P\bar{1}$	$P\bar{1}$	$P\bar{1}$
a, Å	11.922(2)	11.953(2)	12.663(3)	11.971(2)
b, Å	12.941(3)	12.003(2)	13.569(3)	13.830(3)
c, Å	12.986(3)	13.222(2)	15.350(3)	14.862(3)
α, deg	118.08(3)	66.55(2)	79.68(3)	84.88(3)
β, deg	98.90(3)	76.09(2)	89.67(3)	75.09(3)
γ, deg	91.28(3)	89.98(2)	86.59(3)	65.18(3)
V, Å^3	1736.0(6)	1679.5(5)	2590.2(9)	2157.6(7)
Z	1	1	2	2
ρ_{calcd}, g cm^{-3}	1.505	1.528	1.583	1.451
2*θ* range, deg	50.70	51.36	51.18	51.30
GOF	0.98	1.05	0.91	0.99
*R*1/w*R*2	0.032/0.083	0.028/0.078	0.036/0.084	0.042/0.11

crystal of **1**·2H_2O was also obtained by slow evaporation of its MeCN solution (Experimental Section). The crystallographic data of these crystals are listed in Table 1; their ORTEP drawings and selected bond distances and angles are depicted in Figures S1−S4 in the Supporting Information. Figures 1 and 2 show the structures of the complex cations for **1**·2MeOH, **2**, and **3**·3.5H_2O as examples.

The dinuclear complex **1**·2MeOH contains two bridging tetradentate PY5 and two four-coordinate Ag^I both related by a crystallographic center of symmetry, and has two types of Ag−N bonds: one with distances of 2.234(16) Å (Ag1−N2) and 2.237(19) Å (Ag1−N5*) comparable to those in bis-monopyridine Ag^I complexes $[Ag(4\text{-R-py})_2]^+$ (R = CN: 2.214(4), 2.203(4) Å, R = COPh: 2.146(3), 2.147(3) Å)[10a] and $[Ag(2,6\text{-Mes}_2py)_2]^+$ (2.128(5), 2.132(5) Å, 2,6-Mes_2py = 2,6-bis(mesityl)pyridine),[10b] the other with substantially longer distances of 2.513(29) Å (Ag1−N1) and 2.509(61) Å (Ag1−N4*) comparable to those of 2.470(7)−2.562(8) Å in $[Ag(dotete)]^+$ (dotete = 1,4,7,10-tetrakis(2-(methylsulfanyl)ethyl)-1,4,7,10-tetraazacyclododecane).[11] The Ag1−N2 and Ag1−N5* bonds make an angle of 177.28(9)° (N2−Ag1−N5*), similar to the N−Ag−N angles in linear bis-monopyridine Ag^I complexes (162.2(2)°, 175.3(1)°;[10a] 178.1(2)°[10b]), but a much smaller angle of 91.47(8)° (N1−Ag1−N4*) is formed between the Ag1−N1 and Ag1−N4* bonds.

Similar structures were observed for crystals **1**·2H_2O (Figure S2 in the Supporting Information) and **2** (part a of Figure 2). The unit cell of **2** contains two independent molecules (a and b) with slightly different bond distances and angles (caption of Figure S3 in the Supporting Information). As **1** and **2** each have two normal Ag−N bonds in an angle close to 180°, along with two relatively long Ag−N bonds, the Ag^I ions in these complexes can be described to adopt a 2 + 2 coordination mode, that is a dominating linear, diagonal coordination (as in bis-monopyridine Ag^I complexes[10]) plus weak coordination with two additional pyridyl groups.

Both **1** and **2** feature a unique cyclic metalladecapyridine, whose 10 pyridyl groups are fused on a quadruply branched 28-membered $C_{16}N_{10}Ag_2$ metallamacrocycle core (for example, Figure 1) from which 16, 20-membered $C_{12}N_6Ag_2$ rings in various conformations can be defined. Such a quadruply branched $C_{16}N_{10}M_2$ metallamacrocycle core, to the best of our knowledge, has not previously been observed in the X-ray crystal structures of metal−organic assemblies, although an analogous quadruply branched $C_{16}N_{10}Cu_2$ metallamacrocycle that contains 20-membered $C_{12}N_6Cu_2$ rings in a Cu^{II}-(aliphatic pentaamine) complex, $[Cu^{II}_2(ditame)_2]^{4+}$ (ditame = 2,2,6,6-tetrakis(aminomethyl)-4-azaheptane), was proposed on the basis of molecular mechanics calculations.[12]

Whereas the crystal structures of **1**·2MeOH, **1**·2H_2O, and **2** share a quadruply branched metallamacrocycle core in common, their intramolecular $Ag^I\cdots Ag^I$ distances of 3.911(78), 3.447(45), and 4.060(65) (average) Å, respectively, are considerably different, reflecting that the cavity of the metallamacrocycle is quite flexible. The $Ag^I\cdots Ag^I$ distance in $[Ag^I_2(PY5)_2]^{2+}$ can be affected by the counteranions. We prepared $[Ag^I_2(PY5)_2](CF_3SO_3)_2$ and $[Ag^I_2(PY5)_2](BF_4)_2$ by treatment of PY5 with $Ag(CF_3SO_3)$ and $AgBF_4$, respectively, in a manner similar to that for the preparation of **1**. The structures of the two complexes determined by X-ray crystal analysis (Table S1 and Figures S5 and S6 in the Supporting Information) resemble those of **1** and **2** but show a different intramolecular $Ag^I\cdots Ag^I$ distance of 3.670(18) Å for $[Ag^I_2(PY5)_2](CF_3SO_3)_2$·2MeOH and 3.830(29) Å for $[Ag^I_2(PY5)_2](BF_4)_2$. The long $Ag^I\cdots Ag^I$ distances of >3.44 Å (the sum of the van der Waals' radius of two silver atoms[13]) indicate the absence of $Ag^I\cdots Ag^I$ interaction in these quadruply branched metallamacrocycles.

Recently, Reger and co-workers reported tetradentate arene-linked bis(pyrazolyl)methane complexes $[Ag^I_2(L_m)_2](X)_2$ (L_m = *m*-bis(bis(1-pyrazolyl)methyl)benzene; X = BF_4, PF_6) that also contain a quadruply branched 28-membered

(10) (a) Gotsis, S.; White, A. H. *Aust. J. Chem.* **1987**, *40*, 1603–1608. (b) Bosch, E.; Barnes, C. L. *Inorg. Chem.* **2001**, *40*, 3234–3236.
(11) Gyr, T.; Mäcke, H. R.; Hennig, M. *Angew. Chem., Int. Ed. Engl.* **1997**, *36*, 2786–2788.
(12) Hegetschweiler, K.; Maas, O.; Zimmer, A.; Geue, R. J.; Sargeson, A. M.; Harmer, J.; Schweiger, A.; Buder, I.; Schwitzgebel, G.; Reiland, V.; Frank, W. *Eur. J. Inorg. Chem.* **2003**, 1340–1354.
(13) Bondi, A. *J. Phys. Chem.* **1964**, *68*, 441–451.
(14) (a) Reger, D. L.; Watson, R. P.; Smith, M. D. *Inorg. Chem.* **2006**, *45*, 10077–10087. (b) Canty, A. J.; Engelhardt, L. M.; Healy, P. C.; Kildea, J. D.; Minchin, N. J.; White, A. H. *Aust. J. Chem.* **1987**, *40*, 1881–1891.

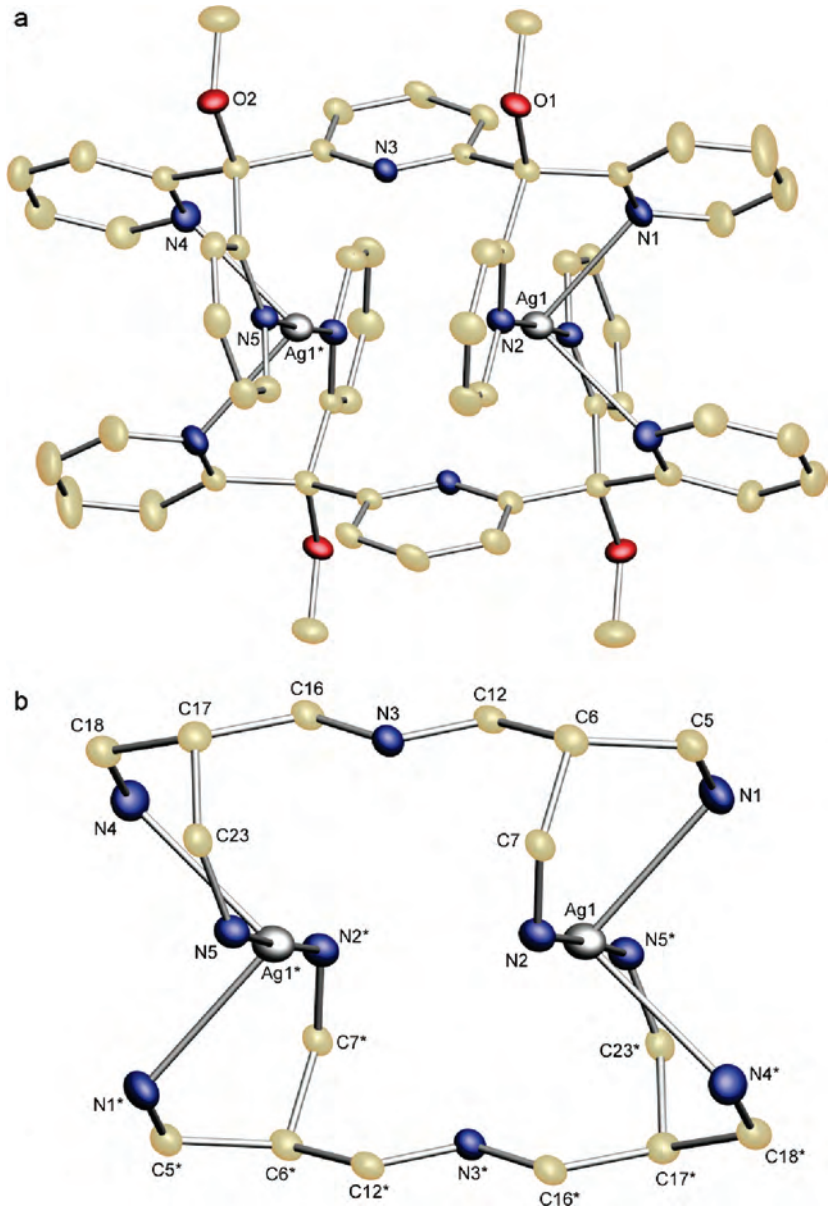

Figure 1. Structure of **1** (a) and its quadruply branched metallamacrocycle core (b) with omission of hydrogen atoms and counteranions.

metallamacrocycle core.[14a] This metallamacrocycle also features a $Ag^I \cdots Ag^I$ distance dependent on the counteranion but consists of $C_{10}N_{16}Ag_2$ integrated with 8 pyrazolyl groups and can be considered as a cyclic metallaoctapyrazole. Compared with the PY5 or PY5-OH analogues, the metallamacrocycles in $[Ag^I_2(L_m)_2](X)_2$ have longer $Ag^I \cdots Ag^I$ distances (5.31 Å for X = BF_4, 4.83 Å for X = PF_6) and show less-varied Ag−N distances and N−Ag−N angles (2.239(4)−2.382(4) Å and 85.47(14)−152.27(14)° for X = BF_4, 2.235(3)−2.424(4) Å and 84.11(13)−158.54(13)° for X = PF_6),[14a] indicating a marked distortion of the Ag^I coordination geometry in the cyclic metallaoctapyrazoles from the above-mentioned 2 + 2 geometry in the metalladecapyridines toward a tetrahedral geometry. A comparison of the structural features of $[Ag^I_2(L_m)_2](BF_4)_2$ and $[Ag^I_2(PY5)_2](BF_4)_2$ is given in the Supporting Information (Figure S7).

The mononuclear **3** contains a four-coordinate Ag^I and two uncoordinated 2-pyridyl groups (part b of Figure 2), with Ag^I−N distances falling within a narrow range of 2.418(61)−2.454(29) Å, comparable to the relatively long Ag^I−N distances of 2.457(37)−2.488(44) Å in **2**. The PPh_3 is coordinated trans to the 2,6-pyridyl group, with a P1−Ag1−N3 angle of 160.41(19)° and a Ag^I−P distance of 2.409(22) Å, and the latter is similar to that reported for $[Ag^I(PPh_3)_2]BF_4$ (2.4177(12) and 2.4219(13) Å).[15] The four-coordinate geometry of Ag^I in **3** can be related to that of Cu^I in the cation $[Cu^I(L)(NCMe)]^+$ (L = 2,6-bis(1-phenyl-1-(pyridin-2-yl)ethyl)pyridine, a tridentate ligand) previously reported by Canty and co-workers,[14b] although this Cu^I complex exhibits a considerably smaller distortion from idealized tetrahedral geometry.

Spectroscopy and Solution Behavior. To ascertain whether the cyclic metalladecapyridines **1** and **2** remain intact

(15) Bachman, R. E.; Andretta, D. F. *Inorg. Chem.* **1998**, *37*, 5657–5663.

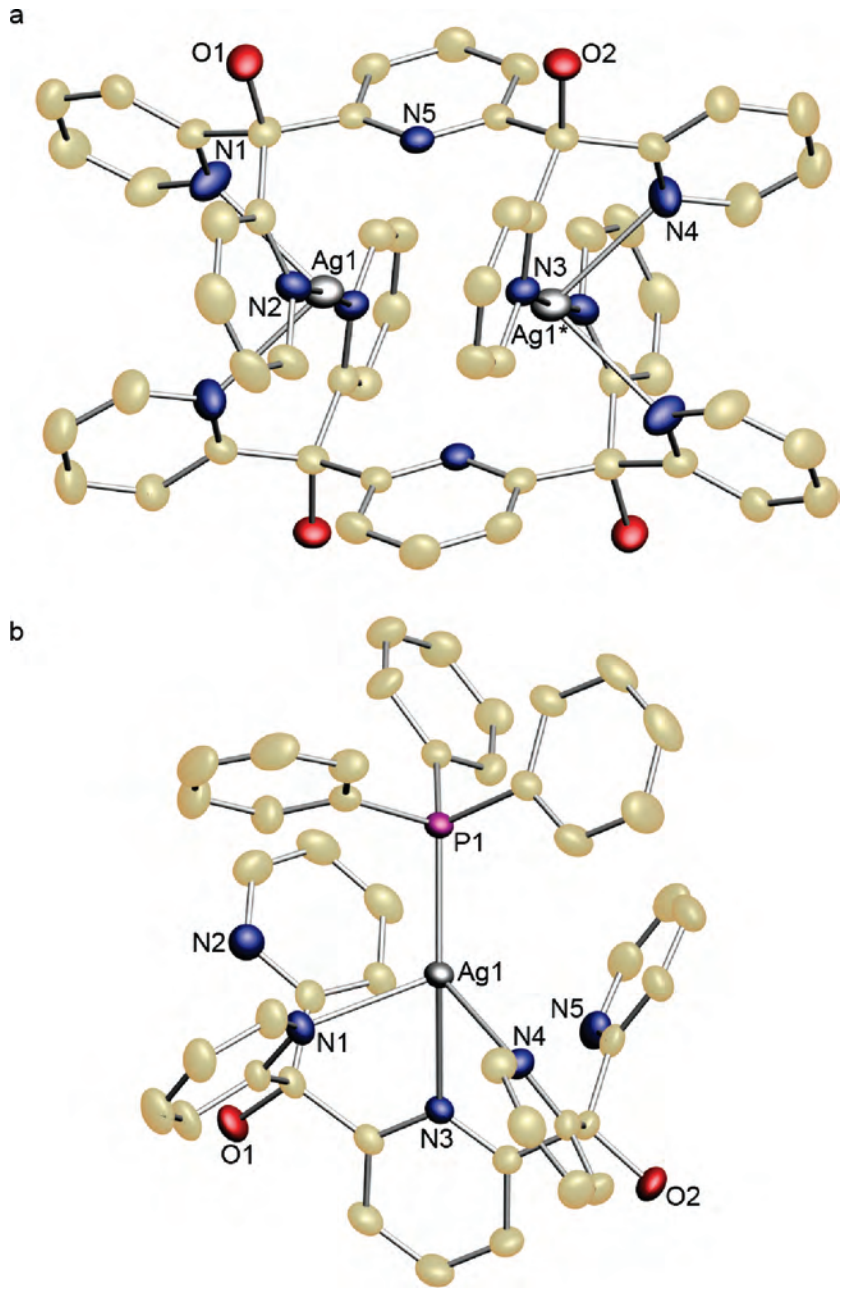

Figure 2. Structures of (a) **2** and (b) **3** with omission of hydrogen atoms and counteranions.

in solution, we measured the room temperature ^{1}H NMR spectra of the two complexes both in MeCN-d_3 and in MeOH-d_4. In each case, the spectrum in MeCN-d_3 is strikingly different from that in MeOH-d_4 (Figure 3 for **1** and Figure S8 in the Supporting Information for **2**). For example, the spectrum of **1** in MeCN-d_3 (part b of Figure 3), like those of mononuclear complexes **I**,[2–4] shows a single set of PY5 signals, which is significantly downfield from those of the free ligand (cf. parts a and b of Figure 3) and assignable to four identical 2-pyridyl groups (H^{c-f}) per 2,6-pyridyl group ($H^{a,b}$). The spectrum of **1** in MeOH-d_4 (part c of Figure 3) consists of two sets of PY5 signals: one is similar to the spectrum in MeCN-d_3 and significantly downfield from the signals of free PY5 in MeOH-d_4, the other features two markedly different sets of 2-pyridyl groups in a 1:1 ratio (the signals in Figure 3 were assigned on the basis of the ^{1}H−^{1}H COSY and NOESY NMR spectra at 0 °C depicted in Figures S9 and S10 in the Supporting Information). We assign the spectrum in MeCN-d_3 (part b of Figure 3) to a mononuclear species $[Ag^I(PY5)(MeCN\text{-}d_3)]^+$, whereas the spectrum in MeOH-d_4 (part c of Figure 3) to two species: $[Ag^I(PY5)(MeOH\text{-}d_4)]^+$ and **1** (note the presence of two different types of 2-pyridyl groups in the crystal structure of **1**). Apparently, **1** was converted into a mononuclear species $[Ag^I(PY5)(MeCN)]^+$ upon dissolving in MeCN at room temperature, but in MeOH a considerable amount of **1** remains intact.

We propose that there is an equilibrium between the di- and mononuclear species in MeOH. Such an equilibrium is supported by the following lines of evidence: (i) Variable-temperature ^{1}H NMR measurements revealed a decrease in the amount of **1** with increasing temperature and vice versa

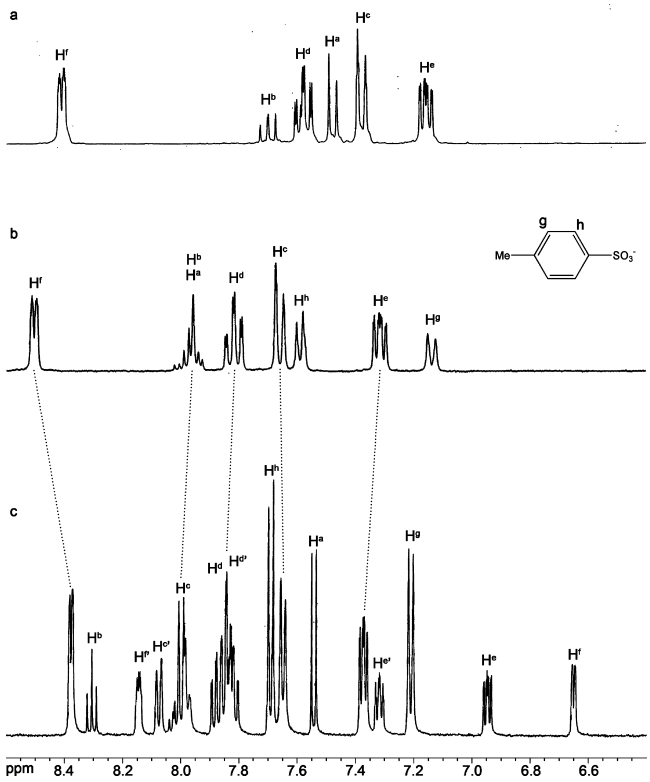

Figure 3. Room-temperature ^{1}H NMR spectra of (a) PY5 in MeCN-d_3 (400 MHz), (b) **1** in MeCN-d_3 (300 MHz), and (c) **1** in MeOH-d_4 (500 MHz). Only the spectra in the aromatic region are shown. The OMe signal of PY5 appears as a sharp singlet for (a) and (b) but two sharp singlets at δ 3.14 and 3.07 ppm in about 1:1 ratio for (c). The labeling schemes for the protons in PY5 and in the complex cation are depicted in Scheme 1.

(Figure 4, also compare part c of Figure 3 with Figure S9 in the Supporting Information). (ii) ^{1}H−^{1}H EXSY NMR spectrum of **1** in MeOH-d_4 at 0 °C (Figure 5) shows cross signals between the corresponding pyridyl protons of the mononuclear species and **1**, indicating an exchange of PY5 coordination between the two complexes. Similar phenomena were observed for **2**.

The FAB mass spectrum of a solution of **1** exhibits a weak cluster peak at *m*/*z* 1337 attributable to $\{[Ag^I_2(PY5)_2](p\text{-}MeC_6H_4SO_3)\}^+$ (Figure 6), along with an intense cluster peak at *m*/*z* 582 ascribable to $[Ag^I(PY5)]^+$ (Figure S11 in the Supporting Information), regardless of whether the sample was dissolved in MeOH or MeCN (the case of **2** is similar). This suggests that, although **1** or **2** was not detected in their MeCN solution by ^{1}H NMR spectroscopy, even at −40 °C (further lowering the temperature made the solvent frozen), a small amount of **1** or **2** could remain intact in the MeCN solution unless the dinuclear species such as $\{[Ag^I_2(PY5)_2](p\text{-}MeC_6H_4SO_3)\}^+$ detected by mass spectrometry came from a dimerizaton of the mononuclear species such as $[Ag^I(PY5)(MeCN)]^+$ in the gas phase upon loss of the solvent molecule.

As mentioned above, slow evaporation of a solution of **1** in MeCN at room temperature afforded crystals of $[Ag^I_2(PY5)_2](p\text{-}MeC_6H_4SO_3)_2\cdot 2H_2O$ (**1**·2H$_2$O), instead of $[Ag^I(PY5)(MeCN)](p\text{-}MeC_6H_4SO_3)$. This could be due to a lower solubility of **1** and the existence of an equilibrium between $[Ag^I(PY5)(MeCN)]^+$ and **1** in MeCN solution,

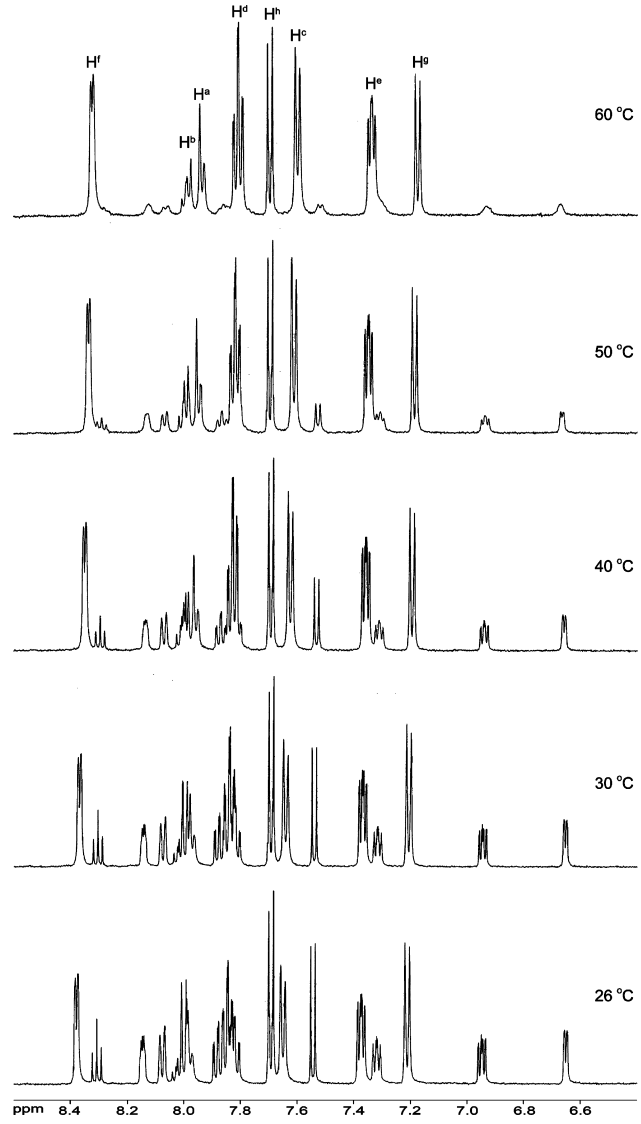

Figure 4. Variable-temperature ^{1}H NMR spectra (500 MHz, aromatic region) of **1** in MeOH-d_4. Only the signals of the counteranion and the mononuclear species generated in the solution are labeled.

although the concentration of **1** in the solution may not be significant. It seems that the binding of MeCN to Ag^I is not strong enough to allow isolation of the mononuclear Ag^I−PY5 complex.

Addition of 2 equiv of PPh_3 to a solution of **1** in MeOH at room temperature resulted in the immediate formation of $[Ag^I(PY5)(PPh_3)](p\text{-}MeC_6H_4SO_3)$, as revealed by ^{1}H NMR spectroscopy (part a of Figure S12 in the Supporting Information). The structure of this mononuclear complex should be similar to that of **3**. An immediate formation of **3** was observed upon treating **2** with 2 equiv of PPh_3 in MeOH. The isolation of **3** in pure form reveals that PPh_3 strongly binds to Ag^I, which prevents the dimerization of the mononuclear species in the course of crystallization.

A proposed diagram showing the interaction of **1** and **2** with PPh_3, MeOH, and MeCN to generate mononuclear species is depicted in Figure 7, wherein the structures of the mononuclear species in the solutions were proposed on the basis of the X-ray crystal structure of **3**. It is noteworthy that, although these mononuclear species such as **3** each

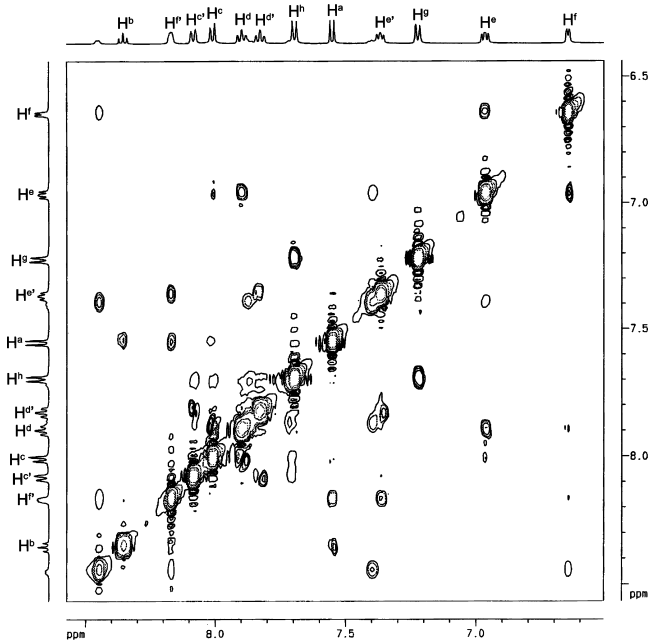

Figure 5. ^{1}H−^{1}H EXSY NMR spectrum (500 MHz, aromatic region) of **1** in MeOH-d_4 at 0 °C. The unlabeled proton resonances arose from the mononuclear species generated in the solution, the assignment of which is similar to that in parts b and c of Figure 3 and Figure 4.

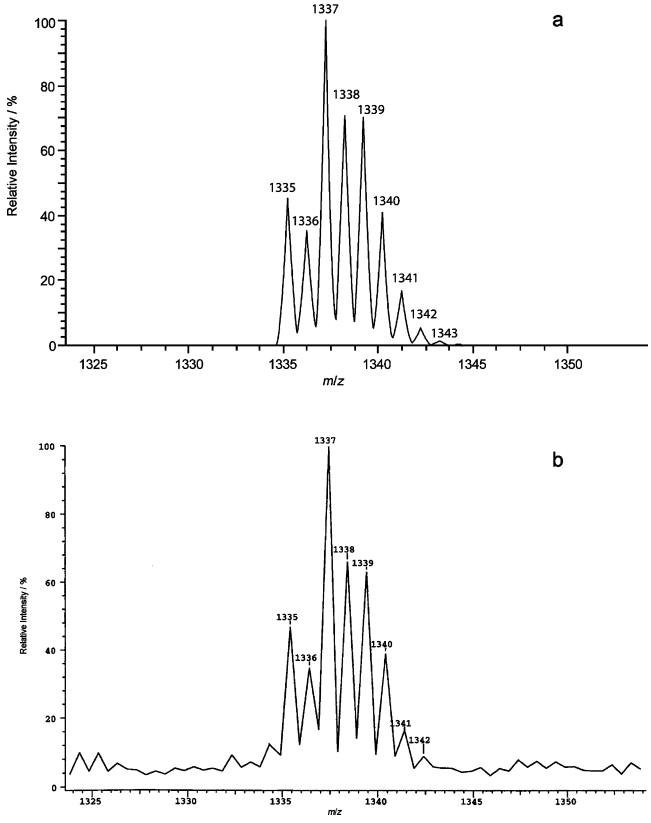

Figure 6. Simulated (a) and observed (b) isotope distributions for the weak peak at *m*/*z* 1337 attributed to $\{[Ag^I_2(PY5)_2](p\text{-}MeC_6H_4SO_3)\}^+$ in the mass spectrum of **1** in MeOH.

contain two different sets of 2-pyridyl groups, their ^{1}H NMR spectra all show only a single set of 2-pyridyl signals (parts b and c of Figure 3, Figure 4; parts c and d of Figure S8, and part a of Figure S12 in the Supporting Information). A

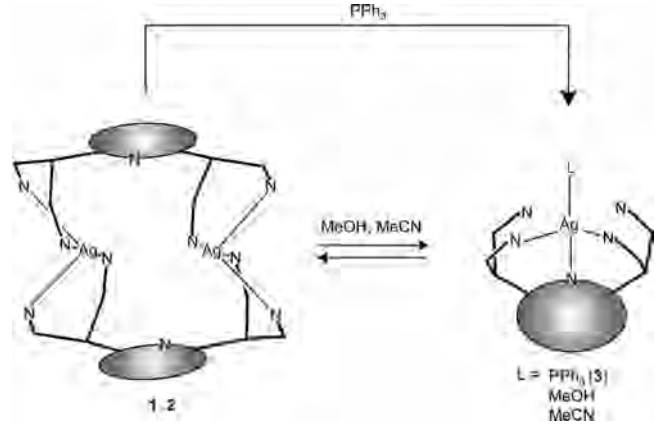

Figure 7. Proposed diagram showing the interaction of **1** and **2** with PPh_3, MeOH, and MeCN (the charges of the complex cations are not shown).

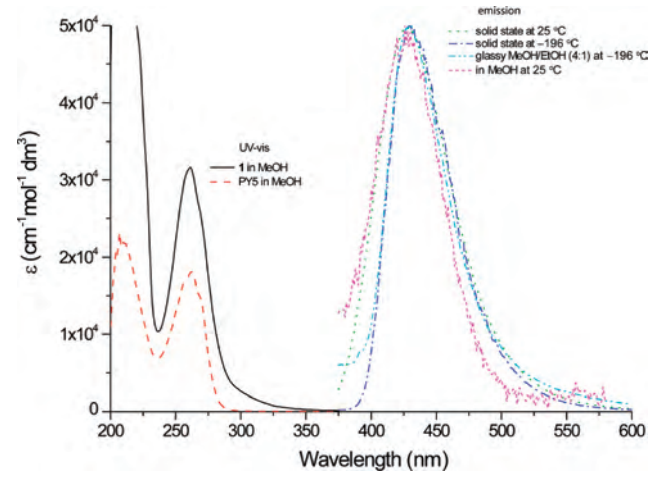

Figure 8. UV−vis absorption spectra (in MeOH) of **1** (2×10^{-5} M) and PY5 (1×10^{-4} M) and emission spectra ($\lambda_{ex} = 300$ nm) of **1** (2×10^{-5} M) in MeOH (at 25 °C, $\tau < 0.001$ μs), solid state (at 25 and −196 °C, $\tau = 3.5$ and 31.2 μs, respectively), and MeOH/EtOH (1:1) glassy solution (at −196 °C, $\tau = 40.0$ μs). The maximum intensities of the emission spectra are normalized.

rationalization is that these mononuclear species are labile in solution, with an exchange of PY5 or PY5-OH between the coordinated and uncoordinated states being rapid on the NMR time scale, analogous to the rationalization by Reger and co-workers for the ^{1}H NMR spectra of $[Ag^I_2(L_m)_2](X)_2$.[14a] Indeed, upon the addition of free PY5 or PY5-OH (2 equiv) to a solution of $[Ag^I(PY5)(PPh_3)](p\text{-}MeC_6H_4SO_3)$ or **3** in MeOH-d_4 at room temperature, a dramatic broadening of the PY5 or PY5-OH proton resonances was observed (for example, part b of Figure S12 in the Supporting Information). Addition of free PY5 (2 equiv) to a solution of **1** in MeCN-d_3 at room temperature appreciably broadened and upfield shifted the PY5 signals (Figure S13 in the Supporting Information). The exchange between the coordinated and uncoordinated PY5 in the solution of **1** in MeCN-d_3 is still rapid upon lowering the temperature to −40 °C. In contrast, no change was observed for the PY5 signals of $[Ag^I_2(PY5)_2]^{2+}$ in MeOH-d_4 solution of **1** at room temperature upon the addition of free PY5 (2 equiv); only those of the proposed $[Ag^I(PY5)(MeOH\text{-}d_4)]^+$ generated in the solution were appreciably upfield shifted (Figure S14 in the

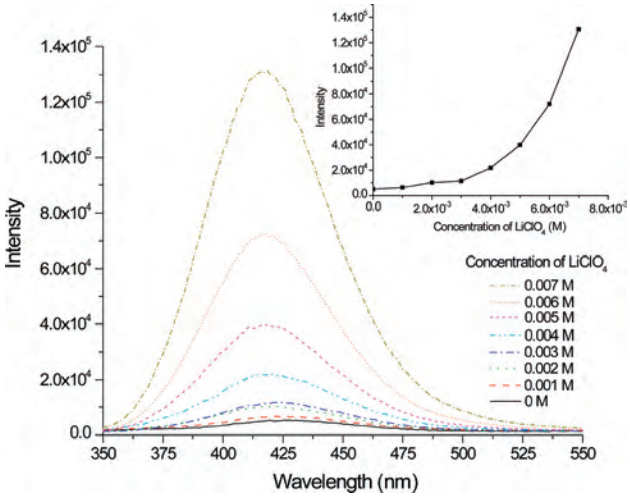

Figure 9. Emission spectra (λ_{ex} = 300 nm) of **1** (1×10^{-4} M) in MeOH at 25 °C upon the addition of different amounts of $LiClO_4$.

Supporting Information), revealing that the metallamacrocyle of **1** is not labile in MeOH solution at room temperature on the NMR time scale.

We also measured the UV−vis absorption and emission spectra of **1** in MeOH at 25 °C (Figure 8). The UV−vis absorption spectrum shows a band at λ_{max} 261 nm ($\epsilon > 10^4$ dm^3 mol^{-1} cm^{-1}), together with a weak broadband at λ 300−350 nm ($\epsilon \approx 10^3$ dm^3 mol^{-1} cm^{-1}); the former is similar to that of the free PY5 ligand and is assigned to intraligand (IL) transition. The emission spectrum has a band at λ_{max} ~428 nm ($\tau < 0.001$ μs) upon excitation at 300 nm, and the excitation spectrum of this 428 nm emission shows a band at λ_{max} ~300 nm, which is red-shifted from that in the UV−vis absorption spectrum. The λ_{max} of the emission band is nearly identical to that measured in solid state at 25 °C (τ = 3.5 μs) and −196 °C (τ = 31.2 μs) and in MeOH/EtOH (4:1) glassy solution at −196 °C (τ = 40.0 μs). In contrast, $[Ag^{I}(PY5)(PPh_3)](p\text{-}MeC_6H_4SO_3)$ is essentially nonemissive in MeOH solution at 25 °C, although it exhibited an emission band in the solid state with λ_{max} 432 nm at 25 °C (τ = 0.3 μs) and 454 nm at −196 °C (τ = 3 μs) upon excitation at 350 nm. Changing the solvent from MeOH to MeCN rendered the solution of **1** nonemissive but did not significantly alter the UV−vis spectrum.

Interestingly, the emission of **1** in MeOH at room temperature was markedly enhanced by addition of $LiClO_4$ (due possibly to ion pair formation), and a ~25−fold increase in the emission intensity was observed when the concentration of $LiClO_4$ increased from 0 to 0.007 M (Figure 9). Addition of more $LiClO_4$ (total concentration: ≤ 0.008 M) did not result in a further increase in emission intensity, and the solution remained transparent. The particle sizes in the transparent solutions after the addition of $LiClO_4$ are outside the range of 10−5000 nm detectable by dynamic light scattering (DLS) measurements using Zetasizer 3000 HAS (Malvern Instruments). We noted that increase of the $LiClO_4$ concentration to >0.01 M rendered the solution to become a white suspension with an emission at λ_{max} 428 nm. A similar emission enhancement occurred if $NaClO_4$, $[^nBu_4N]ClO_4$, or NH_4PF_6 was used instead of $LiClO_4$, but no emission enhancement was observed upon replacing the additive $LiClO_4$ with LiOTf, NaOTf, NaOAc, $Li(CF_3CO_2)$, NH_4BF_4, sodium succinate, or sodium phosphates (PO_4^{3-}, HPO_4^{2-}, and $H_2PO_4^-$).

Conclusion

We have observed the formation of two new types of metal PY5 or PY5-OH complexes: mono- and dinuclear four-coordinate Ag^I complexes, despite the typical function of PY5 or PY5-OH as a pentadentate mononucleating chelator for generating six-coordinate metal complexes and the previous reports of a number of six-coordinate Ag^I complexes. Chelation of two metal ions by PY5 or PY5-OH forms a unique cyclic metalladecapyridine that features 10 pyridyl groups fused on a quadruply branched 28-membered metallamacrocycle core, which first demonstrates the application of PY5 or PY5-OH in the self-assembly of non-mononuclear metal−organic architectures.

Experimental Section

General. PY5 and PY5-OH were prepared according to the published procedures.[2,4a] ^1H and $^{31}P\{^1H\}$ NMR spectra were collected on a Bruker DPX 300, AV 400, or DRX 500 spectrometer; chemical shifts are relative to tetramethylsilane (^1H NMR) or 85% H_3PO_4 ($^{31}P\{^1H\}$ NMR). FAB mass spectra were measured on a Finnigan MAT 95 spectrometer. UV−vis spectra were obtained on a Hewlett-Packard 8453 diode array spectrophotometer. Emission spectra were measured on a Spex Fluorolog-3 spectrofluorometer. Elemental analyses were performed by the Institute of Chemistry, the Chinese Academy of Sciences.

Isolation of $[Ag^I_2(PY5)_2](p\text{-}MeC_6H_4SO_3)_2$ (1). A solution of $Ag(p\text{-}MeC_6H_4SO_3)$ (27.9 mg, 0.1 mmol) in CH_2Cl_2 (15 mL) was added to a solution of PY5 (47.5 mg, 0.1 mmol) in MeOH (10 mL). The mixture was stirred for 30 min and then evaporated to dryness. The white residue was washed with Et_2O, recrystallized at room temperature by diffusion of Et_2O into the solution in a minimum amount of CH_2Cl_2-MeOH (1:1 v/v), and dried in air. Yield: 90%. A similar yield of **1** was obtained through the reaction of $Ag(p\text{-}MeC_6H_4SO_3)$ with PY5 in MeCN, other than MeOH, followed by recrystallization at room temperature by diffusion of Et_2O into the solution in a minimum amount of CH_2Cl_2. ^1H NMR (300 MHz, MeCN-d_3): δ = 8.50 (d, J = 4.8, 4H), 8.02−7.93 (m, 3H), 7.82 (dt, J = 7.8, 1.7, 4H), 7.67 (d, J = 8.0, 4H), 7.60 (d, J = 8.1 Hz, 2H), 7.34−7.29 (m, 4H), 7.14 (d, J = 8.1, 2H), 3.09 (s, 6H), 2.33 (s, 3H). FAB MS (MeOH): m/z 582 ($\{Ag^I(PY5)\}^+$), 1337 ($\{[Ag^I_2(PY5)_2](p\text{-}MeC_6H_4SO_3)\}^+$). Anal. Calcd for $C_{72}H_{64}Ag_2N_{10}O_{10}S_2 \cdot H_2O$: C, 56.62; H, 4.36; N, 9.17. Found: C, 56.32; H, 4.52; N, 8.97.

Isolation of $[Ag^I_2(PY5\text{-}OH)_2](NO_3)_2$ (2). $AgNO_3$ (17.0 mg, 0.1 mmol) was added to a solution of PY5-OH (44.7 mg, 0.1 mmol) in MeOH (20 mL). The mixture was stirred for 30 min and then evaporated to dryness. The white residue was washed with Et_2O, recrystallized at room temperature by diffusion of Et_2O into the solution in a minimum amount of MeOH, and dried in air. Yield: 90%. ^1H NMR (400 MHz, MeCN-d_3): δ = 8.45 (d, J = 4.1 Hz, 4H), 7.92−7.89 (m, 3H), 7.75 (dt, J = 7.8, 1.8 Hz, 4H), 7.59 (d, J = 7.2 Hz, 4H), 7.30−7.27 (m, 4H), the OH resonances were not located. FAB MS (MeOH): m/z 554 ($Ag(PY5\text{-}OH)]^+$), 1172 $[\{[Ag^I_2(PY5\text{-}OH)_2](NO_3)\}]^+$. Anal. Calcd for $C_{54}H_{42}Ag_2N_{12}O_{10} \cdot H_2O$: C, 51.77; H, 3.54; N, 13.42. Found: C, 51.93; H, 3.80; N, 13.40.

Isolation of $[Ag^{I}(PY5\text{-}OH)(PPh_3)]NO_3$ (3). $AgNO_3$ (17.0 mg, 0.1 mmol) and PPh_3 (26.2 mg, 0.1 mmol) were added to a solution of PY5-OH (44.7 mg, 0.1 mmol) in MeOH (20 mL). After the mixture was stirred for 30 min, the solvent was removed. The white residue was washed with hexane, recrystallized at room temperature by diffusion of Et_2O into the solution in a minimum amount of MeOH, and dried in air. Yield: 88%. ^{1}H NMR (400 MHz, MeOH-d_4): $\delta = 8.26$ (d, $J = 4.9$ Hz, 4H), 7.98−7.88 (m, 3H), 7.62−7.59 (m, 8H), 7.51 (dt, $J = 7.4$, 1.7 Hz, 3H), 7.38 (dt, $J = 7.6$, 1.6 Hz, 6H), 7.08−7.04 (m, 4H), 7.00−6.95 (m, 6H), the OH resonances were not located. ^{31}P{^{1}H} NMR (162 MHz, MeOH-d_4): $\delta = 11.1$ (d, $^1J_{P-Ag} = 607$ Hz). FAB MS (MeOH): *m*/*z* 554 ([Ag(PY5-OH)]$^+$), 816 ([Ag(PY5-OH)(PPh_3)]$^+$). Anal. Calcd for $C_{45}H_{36}AgN_6O_5P\cdot$MeOH: C, 60.60; H, 4.42; N, 9.22. Found: C, 60.24; H, 4.60; N, 8.92.

X-ray Crystal-Structure Determinations of 1·2MeOH, 1·2H$_2$O, 2, and 3·3.5H$_2$O. Diffraction-quality crystals of **1**·2MeOH (0.6 × 0.35 × 0.2 mm^3), **2** (0.35 × 0.2 × 0.1 mm^3), and **3**·3.5H_2O (0.5 × 0.2 × 0.15 mm^3) were obtained by slow diffusion of Et_2O into a solution of the corresponding complex in MeOH at room temperature. A diffraction-quality crystal of **1**·2H_2O (0.6 × 0.3 × 0.2 mm^3) was obtained by slow evaporation, at room temperature, of a MeCN solution of **1** prepared from the reaction of Ag(*p*-$MeC_6H_4SO_3$) with PY5 in MeCN. The crystals were each placed in a glass capillary for data collection at 28 °C (**1**·2H_2O, **3**·3.5H_2O) or −20 °C (**1**·2MeOH, **2**) on a Bruker Smart CCD 1000 diffractometer (**1**·2H_2O), or a MAR diffractometer with a 300-mm image plate detector (for the other crystals), using graphite monochromatized Mo Kα radiation ($\lambda = 0.71073$ Å). The data were collected with 2° oscillation step of φ, 180-s (**1**·2MeOH), 420-s (**2**), and 8-min (**3**·3.5H_2O) exposure time, and scanner distance at 120 mm. A total of 80 (**1**·2MeOH), 100 (**3**·3.5H_2O), and 130 (**2**) images were collected. The images were interpreted, and the intensities were integrated using program *DENZO*.[16] The structure was solved by direct methods employing *SIR-97*[17] (**1**·2MeOH, **3**·3.5H_2O) or *SHELXS-97*[18] (**1**·2H_2O, **2**) program on a PC. Many non-hydrogen atoms including silver, phosphorus, and sulfur were located according to the direct methods and the successive least-squares Fourier cycles. Two nitrogen atoms of the two uncoordinated pyridyl groups in **3**·3.5H_2O were located according to their thermal parameters and the difference Fourier map (no ghost peak attached). For all of the complexes, the positions of other non-hydrogen atoms were found after successful refinement by full-matrix least-squares using the *SHELXL-97* program[19] on a PC. The asymmetric unit consists of half of the formula unit including one *p*-$MeC_6H_4SO_3$ anion and one MeOH molecule for **1**·2MeOH; half of a formula unit including one *p*-$MeC_6H_4SO_3$ anion and one water molecule for **1**·2H_2O; two halves of the molecules including two nitrate anions for **2**; and one formula unit including one NO_3 anion and three-and-a-half water molecules for **3**·3.5H_2O. In the final stage of least-squares refinement, all non-hydrogen atoms were refined anisotropically. Hydrogen atoms (except those on the water oxygen in **1**·2H_2O and **3**·3.5H_2O) were generated by the program *SHELXL-97*. The positions of hydrogen atoms were calculated based on the riding mode with thermal parameters equal to 1.2 times that of the associated carbon atoms and participated in the calculation of final *R*-indices.

Acknowledgment. This work was supported by The University of Hong Kong, the Hong Kong Research Grants Council (HKU 7027/05P), and the University Grants Committee of the Hong Kong SAR of China (Area of Excellence Scheme, AoE/P-10/01).

Supporting Information Available: Details about the X-ray crystal structure determinations of $[Ag^{I}_2(PY5)_2](CF_3SO_3)_2\cdot$2MeOH and $[Ag^{I}_2(PY5)_2](BF_4)_2$ and the CIF files for all the crystal structures reported herein. This material is available free of charge via the Internet at http://pubs.acs.org.

IC8000043

(16) Otwinowski, Z.; Minor, W. In *Methods in Enzymology, Vol. 276: Macromolecular Crystallography*; Carter, C. W., Jr., Sweet, R. M., Eds.; Academic Press: New York, 1997; Part A, pp 307−326.

(17) Altomare, A.; Burla, M. C.; Camalli, M.; Cascarano, G. L.; Giacovazzo, C.; Guagliardi, A.; Moliterni, A. G. G.; Polidori, G.; Spagna, R. *J. Appl. Crystallogr.* **1999**, *32*, 115–119.

(18) Sheldrick, G. M. *SHELXS-97. Program for the Solution of Crystal Structures*; University of Göttingen: Göttingen, Germany, 1997.

(19) Sheldrick, G. M. *SHELXL-97. Program for the Refinement of Crystal Structures*; University of Göttingen: Göttingen, Germany, 1997.